

# Ionic Complexes of Bis(hydroxyarylidene)alkanones with Strong Polymeric Bases as a New Class of Third-Order Nonlinear Optical Chromophores

A. V. Tenkovtsev,<sup>†</sup> A. V. Yakimansky,<sup>†</sup> M. M. Dudkina,<sup>†</sup> V. V. Lukoshkin,<sup>‡</sup>  
H. Komber,<sup>§</sup> L. Häussler,<sup>§</sup> and F. Böhme<sup>\*,§</sup>

*Institute of Polymer Research Dresden e.V., Hohe Strasse 6, 01069 Dresden, Germany,  
Institute of Macromolecular Compounds, Russian Academy of Science, 199004 Bolshoy pr. 31,  
St. Petersburg, Russia, and I. A. Ioffe Physicotechnical Institute, Russian Academy of Science,  
194021 Polytechnicheskaya 27, St. Petersburg, Russia*

*Received November 28, 2000; Revised Manuscript Received July 5, 2001*

**ABSTRACT:** Complex formation of various mono- and bis(hydroxyarylidene)alkanones with poly(1,10-decamethyleneacetamidine) in solution and in the solid phase was investigated by UV/vis and NMR spectroscopy. It could be shown that due to the strong basicity of the polyamidine a deprotonation of the chromophores occurred. This resulted in a significant shift of the longest wavelength absorption band of the chromophores to higher wavelengths. Additionally, third-order nonlinear optical activity was evidenced on solution cast films. Besides the optical properties, the thermal behavior of the mixtures was also influenced by the interactions between the polymer and chromophore. An increase of the glass transition temperature of the polymer of about 60 K was attributed to an ionic network formation. The complexes showed good film-forming properties and sufficiently high thermal stability.

## Introduction

Nonlinear optical (NLO) materials are widely known and used in a number of processes and applications. With the help of such materials it is expected to realize all-optical computing and signal processing. In particular, an increase in the rate of telecommunication by at least 3 orders of magnitude is expected.<sup>1,2</sup> Moreover, the availability of high-frequency laser beams produced by third harmonic generation (THG) processes will lead to tremendous progress in atomic and molecular physics and chemistry.

At present, inorganic crystals such as potassium dideuterium phosphate, lithium and potassium niobates, and  $\beta$ -barium borate are mostly used as NLO media in optical devices. However, during the past two decades, an obvious emphasis has been made on the design of new organic and organometallic compounds for NLO applications.<sup>3–15</sup> Compared to inorganic crystals, organic materials are much cheaper and have comparable or even greater nonresonant susceptibilities and shorter nonlinear response times. In addition, NLO properties of organic compounds may be tuned by varying their chemical structures. Their solubility, and thus processability, may be increased by incorporation of special functional groups.

Highly polarizable  $\pi$ -electron systems of conjugated semiconducting organic polymers have made them attractive candidates with a great potential for third-order NLO applications. An incomplete list of such polymers includes polyacetylenes,<sup>16,17</sup> polydiacetylenes,<sup>18,19</sup> and polythiophenes.<sup>20–22</sup>

Despite the considerable efforts put into the development of these materials over many years, they still suffer from lack of transparency and thermal and environmental stability. Therefore, relatively low molecular weight NLO chromophores are now being designed and realized with enhanced third-order nonlinearities due to special structural features different from merely linear  $\pi$ -conjugation length.<sup>3,23,24</sup> In particular, two-dimensional intramolecular charge transfer upon electronic excitation is now recognized as a very favorable property of NLO chromophores promoting their optical nonlinearities.<sup>3,24–26</sup>

However, incorporation of such NLO chromophores into polymer systems is still a challenge for researchers. It has mostly been done by either simple dispersion of NLO chromophores in polymer matrixes<sup>8</sup> (so-called “guest–host” systems) or covalent bonding of NLO chromophores into polymer backbones or side chains.<sup>27–30</sup> The former approach has an obvious disadvantage due to a probable lack of compatibility of an NLO chromophore with polymer matrixes. As to the latter approach, it could be complicated from the synthetic point of view. Besides, modification of a NLO chromophore chemical structure upon its covalent inclusion into a polymer chain and restriction of its mobility may have unfavorable consequences for NLO properties of the polymer system.

An alternative for such polymers with covalently attached NLO chromophores could be strong noncovalent complexes of low molecular weight NLO compounds and suitable polymer carriers. Following this direction, we recently reported on ionic H-bonded complex formation between the second-order NLO-active 2,6-bis(4-hydroxybenzylidene)cyclohexanone<sup>26</sup> and the strongly basic poly(1,10-decamethyleneacetamidine) (**1**) (Scheme 1).<sup>31</sup>

The second harmonic generation (SHG) effect was not observed at these complexes, probably due to a certain lack of noncentrosymmetric arrangement of chro-

\* To whom correspondence should be addressed. E-mail: Boehme@ipfdd.de.

<sup>†</sup> Institute of Macromolecular Compounds, Russian Academy of Science.

<sup>‡</sup> I. A. Ioffe Physicotechnical Institute, Russian Academy of Science.

<sup>§</sup> Institute of Polymer Research Dresden e.V.

Scheme 1

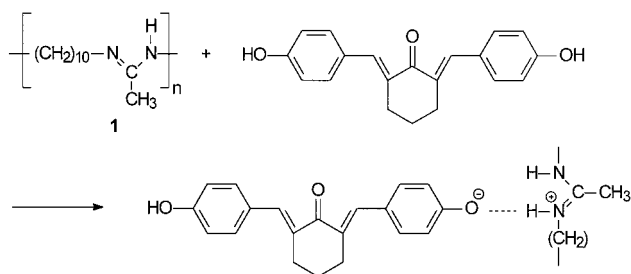
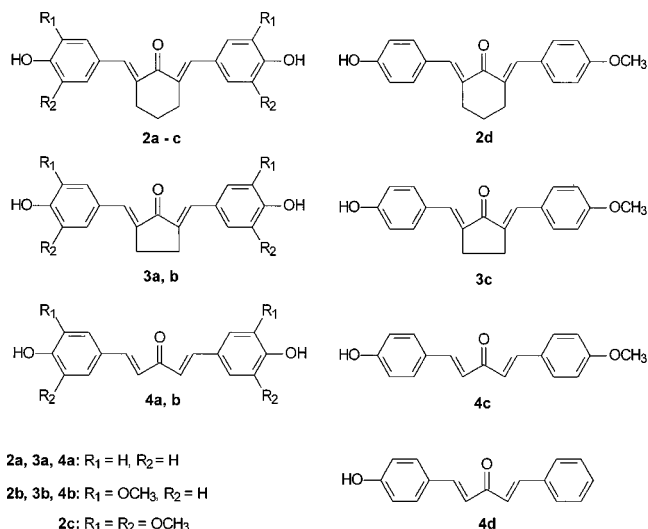


Chart 1



mophores. However, drastic changes in the electronic structure of the chromophore due to ionization and complex formation lead to the appearance of a third-order nonlinear optical effect called THG.

In the present paper, a systematic study of complex formation of various mono- and bis(hydroxyarylidene)-alkanones (Chart 1) with **1** is presented. UV/vis and <sup>1</sup>H and <sup>13</sup>C NMR measurements in solution were performed. Complexes precipitated from solution were characterized by means of solid-state <sup>13</sup>C NMR, DSC, and TGA. THG efficiencies of the complexes were measured on solution cast films.

## Experimental Section

**Materials.** 1,10-Decanediamine, triethylorthoacetate (Fluka), 4-hydroxybenzaldehyde, 4-methoxybenzaldehyde (Aldrich), cyclohexanone, and cyclopentanone (Vekton, Russia) were used without further purification.

**Poly(1,10-decamethyleneacetamidine) (1).** A mixture of 47.5 mmol of 1,10-decanediamine, 50 mmol of triethylorthoacetate, and 40 mmol of acetic acid was heated under nitrogen from 80 to 120 °C with stirring and continuous removal of the resulting alcohol by distillation. Then the pressure was reduced to 5 mbar, and the temperature was raised stepwise to 180 °C within 45 min. After another 135 min the reaction was completed. The structure of the polymer was confirmed by NMR and titration of the amidine groups. The degree of polymerization determined by NMR end group analysis was 19. Data for

**1:** <sup>1</sup>H NMR (CD<sub>3</sub>OD) δ (ppm) = 1.33 (s, 12H, CH<sub>2</sub>), 1.53 (m, 4H, CH<sub>2</sub>), 1.90 (CH<sub>3</sub>, partially deuterated), 3.10 (t, 4H, N-CH<sub>2</sub>).

**Bis(hydroxyarylidene)alkanones 2a-c, 3a,b, and 4a,b.** The bis(hydroxyarylidene)alkanones were synthesized according to Vorländer.<sup>32</sup> The respective benzaldehydes were converted with alkanones in a molar ratio of 2:1 in ethanol solution saturated with HCl. After precipitation in water the

reaction products were filtered off. The crude products were recrystallized twice from ethanol. Structures were confirmed by NMR, IR, and elemental analysis.

Data for **2a:** <sup>1</sup>H NMR (CD<sub>3</sub>OD) δ (ppm) = 1.81 (m, 2H, CH<sub>2</sub>), 2.93 (t, 4H, CH<sub>2</sub>), 6.84 (d, 4H, H<sub>ar</sub>), 7.40 (d, 4H, H<sub>ar</sub>), 7.67 (s, 2H, -CH=).

Data for **2b:** <sup>1</sup>H NMR (CD<sub>3</sub>OD) δ (ppm) = 1.82 (m, 2H, CH<sub>2</sub>), 2.96 (t, 4H, CH<sub>2</sub>), 3.89 (s, 6H, OCH<sub>3</sub>), 6.86 (d, 2H, H<sub>ar</sub>), 7.05 (d, 2H, H<sub>ar</sub>), 7.09 (s, 2H, H<sub>ar</sub>), 7.67 (s, 2H, -CH=).

Data for **2c:** <sup>1</sup>H NMR (CD<sub>3</sub>OD) δ (ppm) = 1.84 (m, 2H, CH<sub>2</sub>), 2.00 (t, 4H, CH<sub>2</sub>), 3.89 (s, 12H, OCH<sub>3</sub>), 6.83 (s, 4H, H<sub>ar</sub>), 7.67 (s, 2H, -CH=).

Data for **3a:** <sup>1</sup>H NMR (CD<sub>3</sub>OD) δ (ppm) = 3.10 (s, 4H, CH<sub>2</sub>), 6.88 (d, 4H, H<sub>ar</sub>), 7.47 (s, 2H, -CH=), 7.53 (d, 4H, H<sub>ar</sub>).

Data for **3b:** <sup>1</sup>H NMR (CD<sub>3</sub>OD) δ (ppm) = 3.13 (s, 4H, CH<sub>2</sub>), 3.92 (s, 6H, OCH<sub>3</sub>), 6.89 (d, 2H, H<sub>ar</sub>), 7.18 (d, 2H, H<sub>ar</sub>), 7.22 (s, 2H, H<sub>ar</sub>), 7.47 (s, 2H, -CH=).

Data for **4a:** <sup>1</sup>H NMR (CD<sub>3</sub>OD) δ (ppm) = 6.84 (d, 2H, H<sub>ar</sub>), 7.06 (d, 2H, -CH=), 7.57 (d, 2H, H<sub>ar</sub>), 7.71 (d, 2H, -CH=).

Data for **4b:** <sup>1</sup>H NMR (CD<sub>3</sub>OD) δ (ppm) = 3.93 (s, 6H, OCH<sub>3</sub>), 6.84 (d, 2H, H<sub>ar</sub>), 7.09 (d, 2H, -CH=), 7.19 (d, 2H, H<sub>ar</sub>), 7.30 (s, 2H, H<sub>ar</sub>), 7.72 (d, 2H, -CH=).

**2-(4-Hydroxybenzylidene)cyclohexanone.** To a solution of 2.25 g (0.02 mol) of 4-hydroxybenzaldehyde and 6 g (0.06 mol) of cyclohexanone in ethanol (20 mL) was added with stirring at 0 °C 8 mL of an aqueous KOH solution (50%). After 12 h the mixture was poured into water and neutralized by diluted acetic acid. 2-(4-Hydroxybenzylidene)cyclohexanone was filtered off and recrystallized twice from an ethanol-water (1:1 v/v) mixture. Yield: 1.5 g (38%).

**2-(4-Hydroxybenzylidene)-6-(4-methoxybenzylidene)-cyclohexanone (2d).** A solution of 2.0 g (0.01 mol) of 2-(4-hydroxybenzylidene)cyclohexanone and 1.6 g (0.012 mol) of 4-methoxybenzaldehyde in 30 mL of ethanol was saturated by dry HCl over 3 h. After 12 h the mixture was poured into 150 mL of water and neutralized by sodium hydrogen carbonate solution. The product was filtered off and recrystallized twice from ethanol. Yield: 1.4 g (45%). Data for **2d:** <sup>1</sup>H NMR (CD<sub>3</sub>OD) δ (ppm) = 1.81 (m, 2H, CH<sub>2</sub>), 2.94 (t, 4H, CH<sub>2</sub>), 3.84 (s, 3H, OCH<sub>3</sub>), 6.85 (d, 2H, H<sub>ar</sub>), 6.99 (d, 2H, H<sub>ar</sub>), 7.41 (d, 2H, H<sub>ar</sub>), 7.48 (d, 2H, H<sub>ar</sub>), 7.68 (s, 2H, -CH=).

**2-(4-Hydroxybenzylidene)cyclopentanone.** A 2 mL sample of dried piperidine was added to the solution of 2.25 g (0.02 mol) of 4-hydroxybenzaldehyde in 5.5 mL of cyclopentanone with stirring at 0 °C. After 12 h the mixture was poured into water and neutralized by diluted acetic acid. 2-(4-Hydroxybenzylidene)cyclopentanone was filtered off and recrystallized twice from an ethanol-water (1:1 v/v) mixture. Yield: 1.2 g (30%).

**2-(4-Hydroxybenzylidene)-5-(4-methoxybenzylidene)-cyclopentanone (3c)** was synthesized by the same procedure as **2d**. Instead of 2-(4-hydroxybenzylidene)cyclohexanone, 2-(4-hydroxybenzylidene)cyclopentanone was used. Yield: 1.16 g (38%).

Data for **3c:** <sup>1</sup>H NMR (CD<sub>3</sub>OD) δ (ppm) = 3.11 (s, 4H, CH<sub>2</sub>), 3.86 (s, 3H, OCH<sub>3</sub>), 6.88 (d, 2H, H<sub>ar</sub>), 7.03 (d, 2H, H<sub>ar</sub>), 7.48 (s, 2H, -CH=), 7.53 (d, 2H, H<sub>ar</sub>), 7.62 (d, 2H, H<sub>ar</sub>).

**1-(4-Hydroxyphenyl)-5-(4-methoxyphenyl)penta-1,4-dien-3-one (4c) and 1-(4-hydroxyphenyl)-5-phenylpenta-1,4-dien-3-one (4d)** were synthesized as described previously.<sup>33</sup>

Data for **4c:** <sup>1</sup>H NMR (CD<sub>3</sub>OD) δ (ppm) = 3.85 (s, 3H, OCH<sub>3</sub>), 6.84 (d, 2H, H<sub>ar</sub>), 6.98 (d, 2H, H<sub>ar</sub>), 7.06 (d, 1H, -CH=), 7.10 (d, 1H, -CH=), 7.58 (d, 2H, H<sub>ar</sub>), 7.66 (d, 2H, H<sub>ar</sub>), 7.71 (d, 1H, -CH=), 7.72 (d, 1H, -CH=).

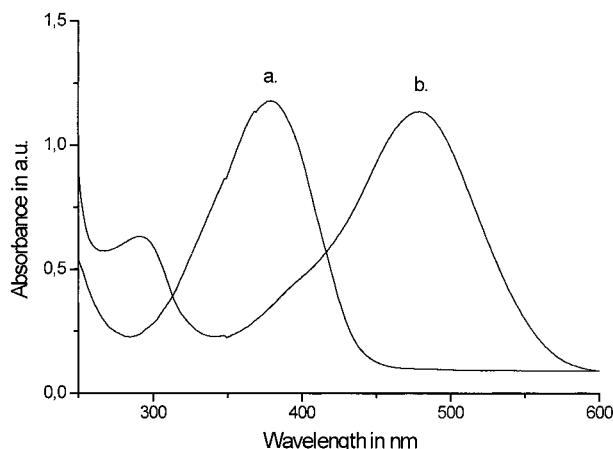
Data for **4d:** <sup>1</sup>H NMR (CD<sub>3</sub>OD) δ (ppm) = 6.84 (d, 2H, H<sub>ar</sub>), 7.07 (d, 1H, -CH=), 7.24 (d, 1H, -CH=), 7.42 (m, 3H, H<sub>ar</sub>), 7.59 (d, 2H, H<sub>ar</sub>), 7.70 (m, 2H, H<sub>ar</sub>), 7.75 (d, 2H, -CH=).

**Complex Preparation.** The polymer-chromophore complexes were prepared by mixing ethanol solutions of the polymer and the chromophore (5% w/w). Samples for NLO experiments were prepared by casting the ethanol solutions of the complexes onto Teflon plates with subsequent evaporation of the solvent at ambient temperature. Before measurements the films were dried in a vacuum (0.1 mmHg). The

**Table 1. Longest Wavelength Absorption Bands of the Chromophores and Their Mixtures with Poly(1,10-decamethyleneacetamidine)<sup>a</sup>**

chromophore	$\lambda_{\text{max}}$ , nm		chromophore	$\lambda_{\text{max}}$ , nm	
	chromophore	mixture		chromophore	mixture
<b>2a</b>	373	468	<b>3c</b>	393	477
<b>2b</b>	387	494	<b>4a</b>	380	478
<b>2c</b>	394	522	<b>4b</b>	394	512
<b>2d</b>	367	453	<b>4c</b>	374	456
<b>3a</b>	417	495	<b>4d</b>	365	457
<b>3b</b>	425	527			

<sup>a</sup> The longest wavelength absorption band of poly(1,10-decamethyleneacetamidine) is about 280 nm.

**Figure 1.** UV/vis spectra of (a) **4a** and (b) a mixture of **4a** with an excess of **1**.

thickness of the films was about 175–200  $\mu\text{m}$ . The films for UV/vis measurements were prepared by spin casting on quartz plates.

**Measurements.** DSC measurements were performed on a Perkin-Elmer DSC 7 at heating and cooling rates of 20 K/min in the temperature range of 60–200  $^{\circ}\text{C}$ . TGA measurements were performed on a Perkin-Elmer TGA 7 in nitrogen within a temperature range of 30–700  $^{\circ}\text{C}$  at a heating rate of 10 K/min. UV/vis spectra were recorded with a Varian Cary 100 spectrometer on ethanol solutions ( $l = 10$  mm) and spin-coated films.

Solution-state NMR experiments were carried out on a Bruker DRX 500 spectrometer operating at 500.13 MHz for  $^1\text{H}$  and 125.75 MHz for  $^{13}\text{C}$ .  $\text{CD}_3\text{OD}$  was used as solvent, lock, and internal standard ( $\delta(^1\text{H}) = 3.31$  ppm;  $\delta(^{13}\text{C}) = 49.0$  ppm). Solid-state NMR data were collected on a Bruker AMX 300 spectrometer operating at 75.47 MHz for  $^{13}\text{C}$  and equipped with a 7 mm CPMAS probe. The spectra were referenced using the CH signal of external adamantane at 38.6 ppm. The measurements were performed with a 6.5  $\mu\text{s}$   $^1\text{H}$  90 $^{\circ}$  pulse duration, a contact time of 1 ms, and a recycle delay of 2 s. A dephasing delay of 45  $\mu\text{s}$  was applied in the dipolar dephasing experiments.<sup>34</sup> The MAS rate was 5 kHz.

The nonlinear optical third-order susceptibilities  $\chi^{(3)}$  were measured by the THG method. The yttrium–neodymium granate (YAG:Nd<sup>3+</sup>) master laser was operated in the Q-switched regime in zero transverse mode TEM<sub>00</sub> at a pulse repetition rate of 14 Hz. Laser pulses, having a wavelength of 1064 nm and a duration time  $\tau_i$  of 15 ns were fed to a single-pass YAG amplifier and amplified up to 30 mJ. P-polarized radiation was focused on a sample by a spherical lens with  $F = 100$  mm. To monitor the intensity of the pulse emitted by the sample, a part of the radiation (about 4%) was split off from the main beam and fed to a precalibrated photodiode. The third harmonic radiation ( $\lambda = 355$  nm) emitted by the sample was collected by the optical system, focused onto the entrance slit of a monochromator, and then recorded by a photomultiplier.

Taking into account the technical difficulties of determining the absolute intensity of the radiation emitted by the sample

with sufficient accuracy, a method was used that relates  $\chi^{(3)}$  and THG intensity values of the sample under investigation to the respective values of a standard sample. In the present work, we used a quartz plate with a thickness of 0.5 mm, graduated on the first maximum of the third harmonic Maker fringes. The following equation is valid:

$$\chi^{(3)} = \chi_s^{(3)} [I^{1/2}(3\omega)/I_c] / [I_s^{1/2}(3\omega)/I_{c,s}]$$

where  $I(3\omega)$ ,  $I_s(3\omega)$  are the THG signal intensities of the sample and the standard, respectively,  $I_c$  and  $I_{c,s}$  are their coherent lengths, and  $\chi_s^{(3)} = 3.11 \times 10^{-14}$  esu for  $\text{SiO}_2$  at  $\lambda = 1.06$  nm.

## Results and Discussion

**Complex Formation of Bis(hydroxyarylidene)-alkanones with Poly(1,10-decamethyleneacetamidine) in Solution.** Recently, it was reported that aliphatic polyamidines exhibit strong basic behavior.<sup>31,35</sup> They are able to interact with proton-donating compounds, resulting in complete deprotonation under certain circumstances. It could be shown that in alcohol solution **1** ( $\text{p}K_a = 10.9$ )<sup>31</sup> forms ionic complexes with 2,6-bis(4-hydroxybenzylidene)cyclohexanone (**2a**). Due to deprotonation of the chromophore the color of the solution changed from pale yellow to deep red. Similar observations were made in the case of the other chromophores studied here (Chart 1). The UV/vis spectra of the chromophores exhibit a bathochromic shift of their longest wavelength absorption band by more than 100 nm (Figure 1, Table 1).

The reason for this is a much stronger linear  $\pi$ -conjugation in the deprotonated chromophores due to a high contribution of the quinoid-like structure compared to the benzenoid-like structures in neutral chromophore molecules (Scheme 2). It should be noted that the same idea of mixing up quinoid- and benzenoid-like resonance structures is realized in squaraine dyes recently employed as NLO chromophores in a PMMA matrix.<sup>24</sup>

As an example, Figure 2 shows the UV/vis spectra of **4b** in the presence of different amounts of poly(1,10-decamethyleneacetamidine). It is seen that, upon increasing the polymer concentration, the intensity of the neutral chromophore absorption band at 394 nm decreases and that of the deprotonated chromophore at 522 nm increases. The presence of an isosbestic point between these two bands demonstrates an equilibrium between the neutral and the deprotonated chromophore, which is shifted toward the deprotonated form upon increasing the relative polymer concentration with respect to that of the chromophore. It is worth mentioning that the maximum absorption of the deprotonated chromophores at these low concentrations is only reached at a high excess of the amidine groups (amidine/hydroxyl group > 15).



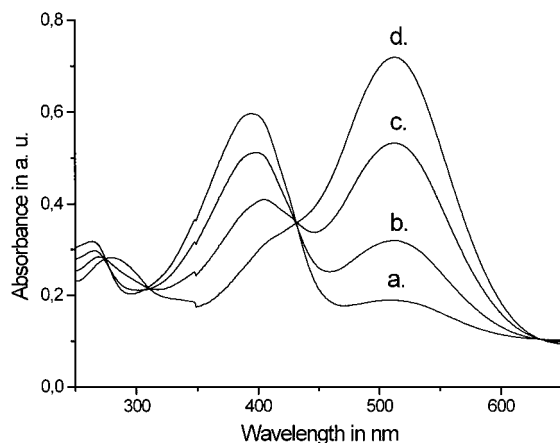
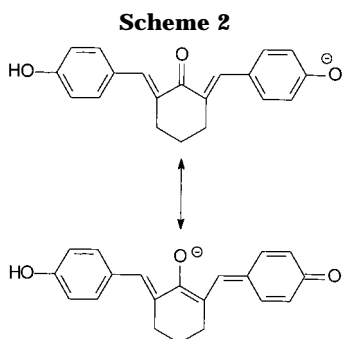


**Figure 2.** UV/vis spectra of **4b** in ethanol in the presence of different amounts of **1** (concentration of **4b**,  $1.47 \times 10^{-5}$  mol/L; molar ratio of hydroxyl groups to amidine groups, (a) 1:0.55, (b) 1:1.35, (c) 1:2.7, (d) 1:5.4).



Stronger bases such as NaOH and KOH exhibit the same bathochromic shift. The UV/vis spectra of the chromophores in the presence of these bases almost coincide with those obtained in the presence of the polyamidine. This clearly shows that the nature of the counterion does not affect the spectra, and thus it has to be assumed that in both cases the deprotonated chromophore anion is formed. Furthermore, the unchanged position of the longest wavelength absorption even at very high base concentrations indicates that this absorption is caused by the doubly deprotonated chromophore. An additional absorption band for the singly deprotonated chromophore has not been found. However, it cannot be excluded that the absorption of the singly deprotonated chromophore is completely overlapped by the doubly deprotonated one. The  $\pi$ -electron conjugation pattern of the singly deprotonated chromophore shown in Scheme 2 should not change significantly after the second deprotonation step. Therefore, similar UV/vis spectra have to be assumed for both chromophore structures. This assumption is supported by the fact that the respective deprotonated monofunctional chromophores adsorb nearly in the same region (e.g., **2c**, **3c**, **4c**, Table 1).

Figure 3 presents  $^1\text{H}$  NMR spectra of **4a** in methanol. The distinct high-field shift of all signals in the presence of a moderate molar excess of polyamidine **1** (amidine/OH group  $\approx 4$ ) clearly indicates deprotonation. Proton exchange processes between the protonated and the deprotonated forms of the chromophores, which are fast on the NMR time scale, render it impossible to detect separate signals for both forms. But, the positions of the appearing averaged signals reflect the degree of deprotonation  $\alpha$ . With increasing  $\alpha$  a progressive shift of all signals is observed.

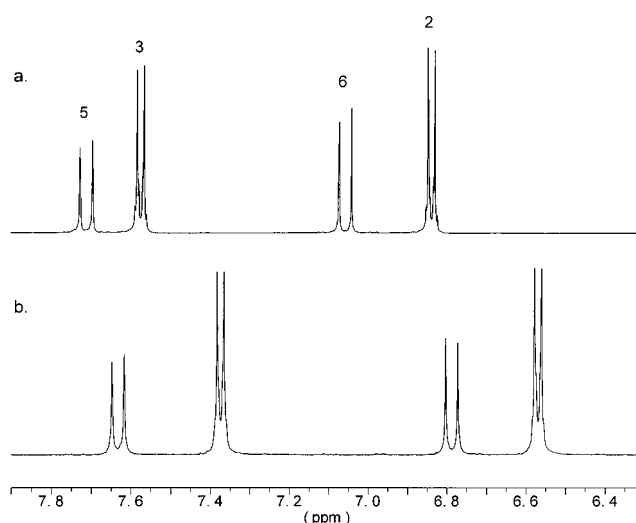


**Figure 3.**  $^1\text{H}$  NMR spectrum of **4a** in ethanol (a) and the pure sample (b) in the presence of a high molar excess of polyamidine **1** (numbering according to Table 3).

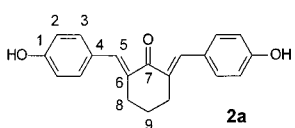
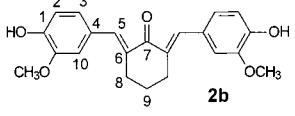
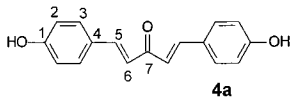
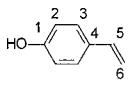
Table 2 summarizes the  $^1\text{H}$  NMR chemical shifts of selected chromophores and of *p*-hydroxystyrene as a model compound as well as the maximum signal shifts  $\Delta\delta$  in the presence of a moderate molar excess of polyamidine **1**. The same maximum signal shifts were observed when a high molar excess of KOH was added ( $\alpha = 1$ ). That allows one to conclude that complete double deprotonation occurs in the presence of both KOH and polyamidine, provided that the concentration of the base is high enough.

The  $^{13}\text{C}$  NMR spectra show similar shift effects due to chromophore deprotonation. The results for **4a**, **4e**, and *p*-hydroxystyrene are summarized in Table 3. For **4a** maximum signal shift effects ( $\alpha = 1$ ) were obtained when a 4-fold excess of amidine groups was added. But, also at nearly equimolar ratios (amidine/OH group = 1.25) a high degree of deprotonation ( $\alpha = 0.95$ ) was observed. This difference from the UV/vis spectroscopic investigations, where a much higher excess of the base was required to get the same effects, can be attributed to the different concentrations at which the measurements had to be carried out.

The different signal shifts  $\Delta\delta$  of the deprotonated forms allow some conclusions to be made regarding their electronic structures. The strongest effect upon addition of base was found for the *ipso*-atoms of the phenolic rings  $\text{C}^1$ , which undergo a low-field shift by more than 12 ppm. This shift is caused by the inductive effect of the negatively charged oxygen and is still detectable at the  $\text{C}^2$  atom. The high-field shift observed at  $\text{C}^4$  and  $\text{C}^6$  is consistent with a considerable quinoidization of the chromophore as shown in Scheme 2. Delocalization of the negative charge through resonance effects causes an increase in the electron density at these atoms and results in negative  $\Delta\delta$  values. The signal shifts of the  $\text{C}^7$ ,  $\text{C}^5$ , and  $\text{C}^3$  atoms are relatively small since resonance stabilization of the charge at these positions is impossible.

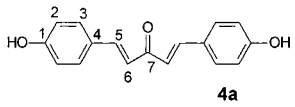
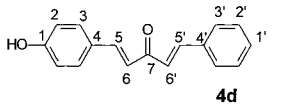
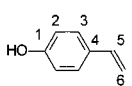
Interestingly, the monofunctional chromophore **4e** responds nearly equally upon deprotonation, so that for the bifunctional chromophore **4a** the influence of the second deprotonation step on the electronic structure is assumed to be negligible. This supports the above assumption that the singly and doubly deprotonated chromophores might absorb in the same UV/vis region.

**Table 2.**  $^1\text{H}$  NMR Chemical Shifts of the Chromophores **2a**, **2b**, and **4a** in the Protonated and Deprotonated Forms in  $\text{CD}_3\text{OD}$ 

structures		$\text{H}^2$	$\text{H}^3$	$\text{H}^5$	$\text{H}^6$	$\text{H}^8$	$\text{H}^9$	$\text{H}^{10}$
 <b>2a</b>	$\delta$ (ppm)	6.84 (d)	7.40 (d)	7.67 (s)	-	2.93 (t)	1.81 (m)	-
	$\Delta\delta^a$	-0.24	-0.12	$\pm 0$	-	-0.03	$\pm 0$	-
 <b>2b</b>	$\delta$ (ppm)	6.86 (d)	7.05 (d)	7.67 (s)	-	2.96 (t)	1.82 (m)	7.09 (s)
	$\Delta\delta^a$	-0.25	-0.06	+0.03	-	-0.01	+0.02	-0.12
 <b>4a</b>	$\delta$ (ppm)	6.84 (d)	7.57 (d)	7.71 (d)	7.06 (d)	-	-	-
	$\Delta\delta^a$	-0.27	-0.20	-0.08	-0.27	-	-	-
	$\delta$ (ppm)	6.73 (d)	7.25 (d)	6.62 (m)	5.55 (d) 5.02 (d)	-	-	-
	$\Delta\delta^a$	-0.18	-0.17	-0.09	-0.20 -0.22	-	-	-

<sup>a</sup> Chemical shift effect in the presence of a high molar excess of polyamidine **1** (deprotonation).

**Table 3.**  $^{13}\text{C}$  NMR Chemical Shifts of **4a**, and **4d** in the Protonated and Deprotonated Forms in  $\text{CD}_3\text{OD}$ 

structure		$\text{C}^1$	$\text{C}^2$	$\text{C}^3$	$\text{C}^4$	$\text{C}^5$	$\text{C}^6$	$\text{C}^7$
 <b>4a</b>	$\delta$ (ppm)	161.55	116.94	131.66	127.75	145.15	123.50	191.72
	$\Delta\delta_p^a$	+12.69	+3.99	+0.65	-6.10	+1.25	-4.08	-0.32
	$\Delta\delta_{\text{KOH}}^b$	+12.58	+3.99	+0.65	-6.02	+1.42	-4.13	+0.07
 <b>4d</b>	$\delta$ (ppm)	161.75	116.97	131.78	127.64	145.84	123.36	191.58
	$\Delta\delta_p^a$	+13.45	+4.13	+1.12	-6.34	+2.88	-4.75	-0.49
	$\delta$ (ppm)	158.42	116.25	128.42	130.78	137.83	110.77	-
	$\Delta\delta_p^a$	+9.54	+3.31	-0.11	-5.22	+1.07	-3.7	-
	$\Delta\delta_{\text{KOH}}^b$	+10.57	+3.68	-0.12	-5.72	+1.12	-3.96	-

<sup>a</sup> Chemical shift effect in the presence of a high molar excess of polyamidine **1**. <sup>b</sup> Chemical shift effect in the presence of an excess of KOH.

Furthermore, a distinct correspondence between the  $\Delta\delta$  values of the chromophores and the model compound *p*-hydroxystyrene was found (Table 3). In comparison to the chromophores *p*-hydroxystyrene possesses only one oxygen on which the negative charge can be localized. Owing to this, it is assumed that the negative charges of the deprotonated chromophores are also mainly localized at the phenolic groups and not at the oxygen in the center of the molecule.

**Complex Formation of Bis(hydroxyarylidene)-alkanones with Poly(1,10-decamethyleneacetamidine) in the Solid State.** UV/vis spectroscopic investigations on spin-cast films should clarify how far complex formations in solution and in the solid phase

are comparable. As an example UV/vis spectra of films of polyamidine **1** with different amounts of chromophore **4a** are shown in Figure 4. Although the absorption bands do not appear as separated as in solution, the influence of deprotonation can be identified by a distinct shift of the absorption maximum and the signal shape indicates an overlap of two bands at about 380 and 500 nm. The maximum of the deprotonated form appears in the same region as in the solution spectra. The spectra show that at an equimolar ratio of amidine and phenolic groups a considerable amount of chromophore is deprotonated. The absorption maxima of the other chromophores in films with polyamidine **1** appear in the same region as found for

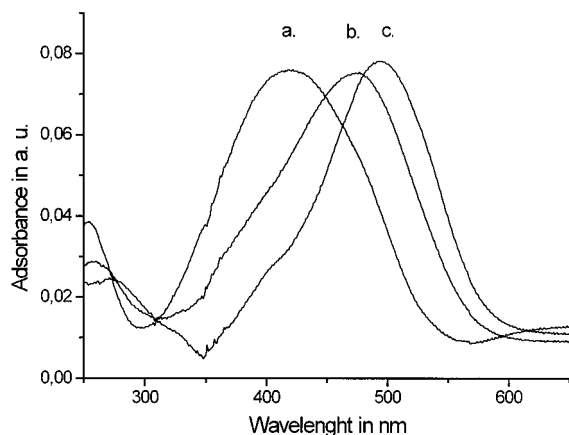


**Figure 4.** UV/vis spectra of solution cast films of chromophore **4a** and polymer **1** (molar ratio of hydroxyl groups to amidine groups, (a) 1:0.5, (b) 1:1, (c) 1:4).

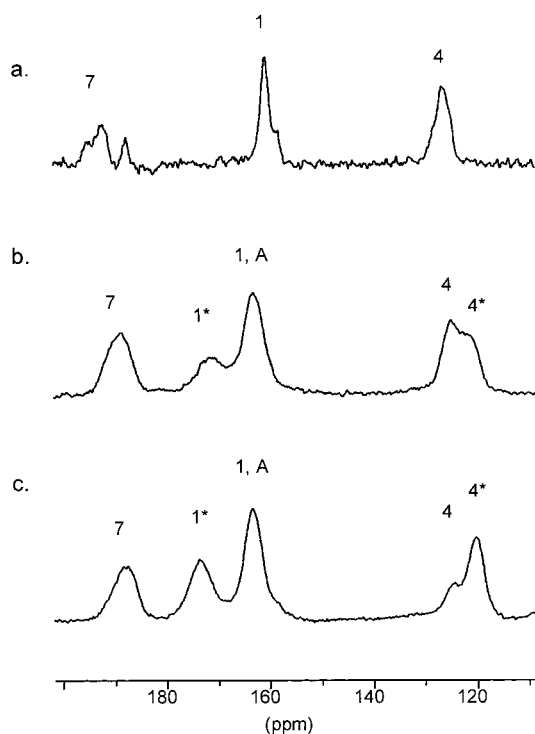


**Figure 5.**  $^{13}\text{C}$  NMR CPMAS spectra (dipolar dephasing experiments) of mixtures of chromophore **4a** and polyamidine **1** (molar ratio of hydroxyl groups to amidine groups, (a) 0:1, (b) 0.5:1, (c) 1:1; \*, signals of deprotonated chromophores; A, signal of the amidine carbon).

the deprotonated chromophores in solution.

Solid-state  $^{13}\text{C}$  NMR CPMAS spectra of **4a** in a complex with **1** are shown in Figure 5. To make the assignment easier, signals of protonated carbon atoms were suppressed by dipolar dephasing.<sup>34</sup> In contrast to the  $^{13}\text{C}$  NMR spectra obtained in solution, signals of the deprotonated and protonated chromophore can be observed. This is caused by more slower or suppressed proton exchange processes in the solid state. Particularly, the ratio of the  $\text{C}^4$  signals at about 125 and 121 ppm, caused by the protonated and deprotonated forms, respectively, clearly shows the increasing content of deprotonated moieties with increasing polyamidine content. In case of the  $\text{C}^1$  atom, the signal of the protonated form is overlapped by the signal of the amidine carbon. However, the intensity change of the  $\text{C}^1$  signal of the deprotonated form at about 174 ppm

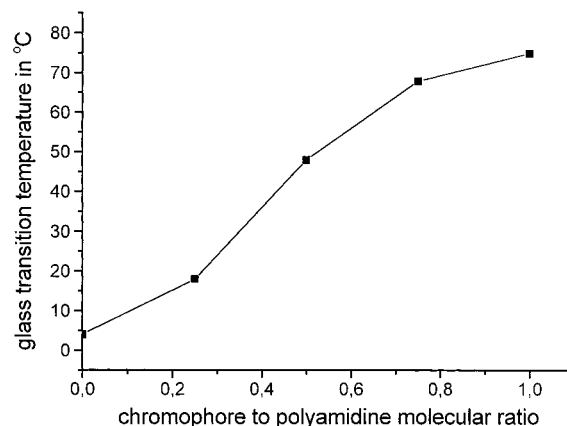


**Figure 6.** Dependency of the glass transition of polymer **1** on the content of chromophore **2a**.

related to the  $\text{C}^7$  signal also indicates the influence of deprotonation.

The differences between the chemical shifts of the protonated and deprotonated forms ( $\Delta\delta$ ) in the solid state ( $\text{C}^1$ , +12.8 ppm;  $\text{C}^4$ , -6.4 ppm) are close to those obtained in solution, showing that the structure in the solid state should not differ much from the one in solution. From the NMR spectra we can estimate that at an equimolar ratio of the phenolic and amidine groups the deprotonated form distinctly predominates in the solid phase.

**Phase Behavior and Thermal Stability.** It was shown earlier<sup>31</sup> that the as-prepared polyamidine **1** is a highly crystalline sample with a melting temperature at about 60 °C. After melting, recrystallization is strongly retarded and polyamidine **1** exhibits only a distinct glass transition at about 5 °C. At ambient temperatures the sample remains in the molten state. In the presence of chromophores the thermal behavior of the polymer changes considerably. As shown for chromophore **2a**, the  $T_g$  values increase with the molar content of the chromophore and tend to level off at chromophore molar amounts higher than 75% (Figure 6). For the pure chromophore no significant transition was found in the investigated range.

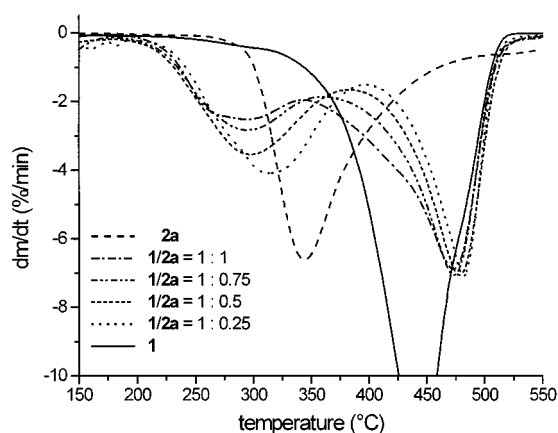
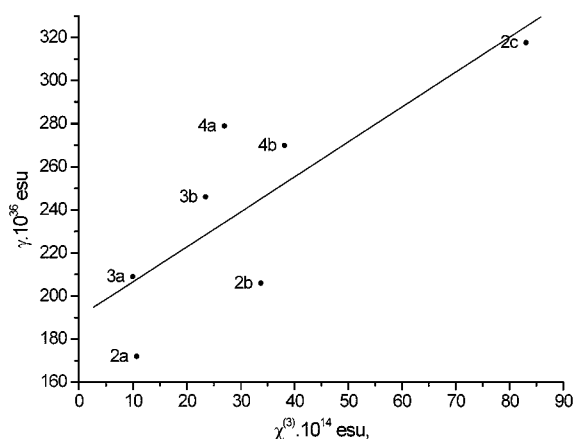
These observations confirm that the products under investigation are not simple mechanical mixtures but new materials with specific properties caused by strong noncovalent intermolecular interactions. Films prepared from these mixtures are stable at ambient temperature over a long time. At a chromophore molar fraction of approximately 30–40% the complexes lose their solubility in alcohol, probably due to a physical network formation.

As evidenced by thermogravimetric (TG) investigations all chromophores were thermostable up to at least 250 °C. Polyamidine **1** showed 1% weight loss at about 230 °C. Also the complexes of the chromophores with polyamidine **1** did not show any decomposition up to at least 200 °C, so that their thermal stability is high enough to resist the possible increase of temperature up to 150–180 °C during the THG measurements caused by the laser beam. As an example, the derivative weight loss curves (DTG) of mixtures of **1** and **2a** at different compositions are shown in Figure 7. The profile of the curves indicates that complexation increases the thermal stability of the polyamidine whereas the thermal stability of the chromophore is reduced.

**Nonlinear Optical Properties of Complexes of Bis(hydroxyarylidene)alkanones with Poly(1,10-**

**Table 4.** THG Efficiencies of Complexes of Poly(1,10-decamethyleneacetamide) with Bis(hydroxyarylidene)alkanones

chromophore	$\chi^{(3)} \times 10^{14}$ (esu), measd	$\gamma \times 10^{36}$ (esu), calcd	chromophore	$\chi^{(3)} \times 10^{14}$ (esu), measd	$\gamma \times 10^{36}$ (esu), calcd
<b>2a</b>	11	172	<b>3b</b>	24	246
<b>2b</b>	34	206	<b>4a</b>	27	279
<b>2c</b>	83	318	<b>4b</b>	38	270
<b>3a</b>	10	209			

**Figure 7.** Derivative curves of the weight loss (DTG) of mixtures of polymer **1** and chromophore **2a**.**Figure 8.** Correlation between the molecular second-order hyperpolarizabilities,  $\gamma$ , calculated for singly deprotonated chromophores by the PM-3 method and measured susceptibilities,  $\chi^{(3)}$ , for films of complexes of different chromophores with polyamide **1**.

**decamethyleneacetamide**). All complexes of bis(hydroxyarylidene)alkanones with the polyamide **1** were found to display third-order NLO effects (THG). The measured susceptibilities  $\chi^{(3)}$  and molecular second-order hyperpolarizabilities  $\gamma$ , calculated by the PM-3 method,<sup>36</sup> are given in Table 4.

It is necessary to point out that neither the pure polyamide nor any of the chromophores show THG effects. Moreover, chromophores incorporated into a PEO matrix are also inactive in THG, although H-bonding between chromophores and the polymer matrix should also occur in this system. Obviously, ionization of the chromophores plays a fundamental role in the THG activity of the complexes studied.

Figure 8 presents the correlation between the measured  $\chi^{(3)}$  and calculated  $\gamma$  values. Both values characterize the magnitude of the THG effects. The latter represents the susceptibility of one molecule. The observed correlation (correlation factor 0.92) confirms the connection of macroscopic optical properties with

structural characteristics on a molecular level. The experimental data show that the introduction of auxochromic (electron-donating) substituents  $R_1$  and  $R_2$  into the benzylidene fragment leads to the enhancement of the THG activity. According to this observation, it is possible to conclude that an increase of the electron density in chromophore molecules amplifies the THG signal.

The structural changes in the chromophore core also affect the NLO activity of the complexes. Complexes of chromophores **2** and **3** which possess a cycloaliphatic central fragment are less THG active than those containing a linear aliphatic spacer between the aromatic moieties. This behavior is probably caused by a lower  $\pi$ -conjugation in the diarylidene cycloalkanone anions. This assumption is supported by quantum-chemical calculations using the PM-3 method. The diarylidene cycloalkanones have a nonflat conformation due to a steric repulsion between the *ortho* protons of the phenyl rings and the methylene protons of the cyclic central fragment, whereas diarylideneacetones have an almost flat conformation.

## Conclusions and Outlook

Complexes of bis(hydroxyarylidene)alkanones with strongly basic poly(1,10-decamethyleneacetamide) have proven to be a new class of ionically bonded polymer systems with a certain potential in third-order NLO applications. One requirement for NLO activity of the chromophores is their deprotonation. It could be evidenced by UV/vis and NMR spectroscopy that in the presence of the aliphatic polyamide **1** deprotonation in the solid phase takes place to a high extent. Obviously, the basicity of the aliphatic polyamide is high enough. In addition, it has to be mentioned that other polymers with lower basicity such as aromatic polyamides or poly(vinylpyridine) do not show this behavior.

Comparative measurements on monofunctional (hydroxyarylidene)alkanones indicate that the optical properties of the bifunctional chromophores are mainly determined by a single deprotonation step. Deprotonation of the second phenyl group takes place but does not influence the absorption behavior significantly. The complexes are thermo- and hydrolytically stable and possess good film-forming properties.

Compared to those of polythiophenes with more complicated architecture,<sup>22</sup> the measured THG efficiencies are smaller. However, the third-order nonlinearities of bis(hydroxyarylidene)alkanones can be considerably increased by modification of their chemical structure. In particular, a distinct increase in third-order nonlinearity for  $\alpha,\omega$ -diphenylpolyenes was found upon introducing electron-withdrawing substituents and increasing the conjugation length.<sup>3,37,38</sup> A similar approach on (hydroxyarylidene)alkanones, which in their deprotonated quinoid-like form are structurally similar to  $\alpha,\omega$ -diphenylpolyenes, is now in progress.



**Acknowledgment.** We thank the Deutsche Forschungsgemeinschaft and the Sächsische Staatsministerium für Wissenschaft und Kunst for financial support.

## References and Notes

- (1) Hinton, H. S. *IEEE Spectrum* **1992**, Feb, 42.
- (2) Bredas, J. L.; Adant, G.; Tackx, P.; Persoons, A. *Chem. Rev.* **1994**, *94*, 243.
- (3) Tykewinski, R. R.; Gubler, U.; Martin, R. E.; Diederich, F.; Bosshard, C.; Günter, P. *J. Phys. Chem. B* **1998**, *102*, 4451.
- (4) *Nonlinear Optics of Organic Molecules and Polymers*; Nalwa, H. S., Miyata, S., Eds.; CRC Press: Boca Raton, FL, 1997.
- (5) *Nonlinear Optical Materials: Theory and Modeling*; Karna, S. P., Yeates, A. Y., Eds.; American Chemical Society: Washington, DC, 1996.
- (6) Zyss, J.; Nicoud, J.-F. *Curr. Opin. Solid State Mater. Sci.* **1996**, *1*, 533.
- (7) Bosshard, C.; Sutter, K.; Prêtre, P.; Hulliger, J.; Flörsheimer, M.; Kaatz, P.; Günter, P. *Organic Nonlinear Optical Materials*; Gordon and Breach: Basel, Switzerland, 1995.
- (8) Special issue: *Chem. Rev.* **1994**, *94*, 1–278.
- (9) Special issue: *J. Opt. Soc. Am. B* **1998**, *15*, 723–932.
- (10) Zyss, J. *Molecular Nonlinear Optics: Materials, Physics and Devices*; Academic Press: Boston, 1993.
- (11) *Organic Materials for Nonlinear Optics II*; Hann, R. A., Bloor, D., Eds.; The Royal Society of Chemistry: Cambridge, 1991.
- (12) Prasad, P. N.; Williams, D. J. *Introduction to Nonlinear Optical Effects in Molecules and Polymers*; Wiley: New York, 1991.
- (13) *Nonlinear Optical Properties of Polymers: Materials Research Society Symposium Proceedings*; Heeger, A. J., Orenstein, J., Ulrich, D. R., Eds.; Materials Research Society: Pittsburgh, PA, 1988; Vol. 109.
- (14) *Nonlinear Optical Properties of Organic Molecules and Crystals*; Chemla, D. S., Zyss, J., Eds.; Academic Press: Orlando, FL, 1987.
- (15) Williams, D. J. *Angew. Chem., Int. Ed. Engl.* **1984**, *23*, 690.
- (16) Hermann, J.-P.; Ducuing, J. *J. Appl. Phys.* **1974**, *45*, 5100.
- (17) Hermann, J.-P.; Ricard, D.; Ducuing, J. *Appl. Phys. Lett.* **1973**, *23*, 178.
- (18) Agrawal, G. P.; Cojan, C.; Flytzanis, C. *Phys. Rev. B* **1978**, *17*, 776.
- (19) Sauteret, C.; Hermann, J.-P.; Frey, R.; Pradère, F.; Ducuing, J.; Baughman, R. H.; Chance, R. R. *Phys. Rev. Lett.* **1976**, *36*, 956.
- (20) Cha, M.; Torruellas, W. E.; Yuan, S. H.; Stegeman, G. I.; Leclerc, M. *J. Opt. Soc. Am. B* **1995**, *12*, 882.
- (21) Torruellas, W. E.; Neher, D.; Zanon, R.; Stegeman, G. I.; Kajzar, F.; Leclerc, M. *Chem. Phys. Lett.* **1990**, *175*, 11.
- (22) Schrof, W.; Rozouvan, S.; Hartmann, T.; Möhwald, H.; Belov, V.; Van Keuren, E. *J. Opt. Soc. Am. B* **1998**, *15*, 889.
- (23) Murata, H.; Izutsu, M. *J. Opt. Soc. Am. B* **1998**, *15*, 884.
- (24) Mathis, K. S.; Kuzyk, M. G.; Dirk, C. W.; Tan, A.; Martinez, S.; Gampos, G. *J. Opt. Soc. Am. B* **1998**, *15*, 871.
- (25) Yakimanski, A. V.; Voigt-Martin, I. G.; Kolb, U.; Matveeva, G. N.; Tenkovtsev, A. V. *Acta Crystallogr., A* **1997**, *53*, 603.
- (26) Voigt-Martin, I. G.; Gao Li; Kolb, U.; Kothe, H.; Yakimansky, A. V.; Tenkovtsev, A. V.; Gilmore, C. *Phys. Rev. B* **1999**, *59*, 6722.
- (27) Martin, R. E.; Gubler, U.; Boudon, C.; Gramlich, V.; Bosshard, C.; Gisselbrecht, J.-P.; Günter, P.; Gross, M.; Diederich, F. *Chem.—Eur. J.* **1997**, *3*, 1505.
- (28) Schreiber, M.; Tykewinski, R. R.; Diederich, F.; Spreiter, R.; Gubler, U.; Bosshard, C.; Poberaj, I.; Günter, P.; Boudon, C.; Gisselbrecht, J.-P.; Gross, M.; Jonas, U.; Ringsdorf, H. *Adv. Mater.* **1997**, *9*, 339.
- (29) Schreiber, M.; Antony, J.; Diederich, F.; Spahr, M. E.; Nesper, R.; Hubrich, M.; Bommeli, F.; Degiorgi, L.; Wachter, P.; Kaatz, P.; Bosshard, C.; Günter, P.; Colussi, M.; Suter, U. W.; Boudon, C.; Gisselbrecht, J.-P.; Gross, M. *Adv. Mater.* **1994**, *6*, 786.
- (30) Cherioux, F.; Audebert, P.; Mailotte, H.; Grossard, L.; Hernandez, F. E.; Lacourt, A. *Chem. Mater.* **1997**, *9*, 2921.
- (31) Böhme, F.; Häussler, L.; Tenkovtsev, A. V.; Yakimansky, A. V. *Polym. Prepr. (Am. Chem. Soc., Div. Polym. Chem.)* **1999**, *40* (2), 1140.
- (32) Vorlander, B. *Ber. Dtsch. Chem. Ges.* **1925**, *58*, 132.
- (33) Di Bella, E. P. (Tenneco Chemicals Inc.). US 3.389.986, 1964.
- (34) Opella, S. J.; Frey, M. H. *J. Am. Chem. Soc.* **1979**, *101*, 5854.
- (35) Böhme, F.; Klinger, C.; Bellmann, C. *Colloids Surf., A* **2001**, *189*, 21.
- (36) Stewart, J. J. P. *J. Comput. Chem.* **1989**, *6*, 791.
- (37) Spangler, C. W.; Havelka, K. O.; Becker, M. W.; Kelleher, T. A.; Cheng, L.-T. *Proc. SPIE—Int. Soc. Opt. Eng.* **1991**, *1560*, 139.
- (38) Cheng, L.-T.; Tam, W.; Stevenson, S. H.; Meredith, G. R.; Rikken, G.; Marder, S. R. *J. Phys. Chem.* **1991**, *95*, 10631.

MA0020234